


# Parity-time symmetric acoustic system constructed by piezoelectric composite plates with active external circuits

Yang Zhou(周扬), Zhang-Zhao Yang(杨彰昭), Yao-Yin Peng(彭尧吟), and Xin-Ye Zou(邹欣晔)
**Citation:**Chin. Phys. B, 2022, 31 (**6**): 064304. DOI: 10.1088/1674-1056/ac4e10
Journal homepage: http://cpb.iphy.ac.cn; http://iopscience.iop.org/cpb

**What follows is a list of articles you may be interested in**

---

## Collision enhanced hyper-damping in nonlinear elastic metamaterial

Miao Yu(于淼), Xin Fang(方鑫), Dianlong Yu(郁殿龙), Jihong Wen(温激鸿), and Li Cheng(成利)
Chin. Phys. B, 2022, 31 (**6**): 064303. DOI: 10.1088/1674-1056/ac48fc

## Impact vibration properties of locally resonant fluid-conveying pipes

Bing Hu(胡兵), Fu-Lei Zhu(朱付磊), Dian-Long Yu(郁殿龙), Jiang-Wei Liu(刘江伟), Zhen-Fang Zhang(张振方), Jie Zhong(钟杰), and Ji-Hong Wen(温激鸿)
Chin. Phys. B, 2020, 29 (**12**): 124301. DOI: 10.1088/1674-1056/abb312

## Using Helmholtz resonator arrays to improve dipole transmission efficiency in waveguide

Liwei Wang(王力维), Li Quan(全力), Feng Qian(钱枫), Xiaozhou Liu(刘晓宙)
Chin. Phys. B, 2019, 28 (**9**): 094301. DOI: 10.1088/1674-1056/ab3447

## A novel multi-cavity Helmholtz muffler

Han-Bo Shao(邵瀚波), Huan He(何欢), Yan Chen(陈岩), Guo-Ping Chen(陈国平)
Chin. Phys. B, 2019, 28 (**5**): 054303. DOI: 10.1088/1674-1056/28/5/054303

## Propagation of acoustic waves in a fluid-filled pipe with periodic elastic Helmholtz resonators

Dian-Long Yu(郁殿龙), Hui-Jie Shen(沈惠杰), Jiang-Wei Liu(刘江伟), Jian-Fei Yin(尹剑飞), Zhen-Fang Zhang(张振方), Ji-Hong Wen(温激鸿)
Chin. Phys. B, 2018, 27 (**6**): 064301. DOI: 10.1088/1674-1056/27/6/064301

---

**RAPID COMMUNICATION**

# Parity–time symmetric acoustic system constructed by piezoelectric composite plates with active external circuits

Yang Zhou(周扬)[1], Zhang-Zhao Yang(杨彰昭)[1], Yao-Yin Peng(彭尧吟)[1], and Xin-Ye Zou(邹欣晔)[1,2,†]

[1] *Key Laboratory of Modern Acoustics, MOE, Institute of Acoustics, Department of Physics, Collaborative Innovation Center of Advanced Microstructures, Nanjing University, Nanjing* 210093, *China*
[2] *State Key Laboratory of Acoustics, Chinese Academy of Sciences, Beijing* 100190, *China*

(Received 5 December 2021; revised manuscript received 31 December 2021; accepted manuscript online 24 January 2022)

Researches on parity-time (PT) symmetry in acoustic field can provide an efficient platform for controlling the travelling acoustic waves with balanced loss and gain. Here, we report a feasible design of PT-symmetric system constructed by piezoelectric composite plates with two different active external circuits. By judiciously adjusting the resistances and inductances in the external circuits, we obtain the exceptional point due to the spontaneous breaking of PT symmetry at the desired frequencies and can observe the unidirectional invisibility. Moreover, the system can be at PT exact phase or broken phase at the same frequency in the same structure by merely adjusting the external circuits, which represents the active control that makes the acoustic manipulation more convenient. Our study may provide a feasible way for manipulating acoustic waves and inspire the application of piezoelectric composite materials in acoustic structures.

**Keywords:** parity-time symmetry, acoustic gain material, piezoelectric composite plate, exceptional point

**PACS:** 43.40.+s, 43.38.Ew, 43.40.Yq **DOI:** 10.1088/1674-1056/ac4e10

## 1. Introduction

Parity–time (PT) symmetry, or space–time reflection symmetry, initially proposed in quantum mechanics by Bender,[1,2] reveals that the quantum systems with non-Hermitian Hamiltonians can still host a real spectrum corresponding to observable physical quantities when they satisfy PT symmetry. After being introduced into optics,[3] PT symmetry has been extensively investigated on the experimental implementation and properties demonstration in the classical wave systems, such as unidirectional zero reflection,[4,5] coherent perfect absorption,[6–8] asymmetric mode conversion,[9,10] power oscillations of light propagation[11] and single-mode laser.[12–14] In the meantime, PT-symmetric acoustics[15] also has attracted intense attention after being proposed by Zhu *et al.* Since it is difficult to find the natural gain material in acoustics,[16] passive PT-symmetric systems[17–19] that consist of purely dissipative elements inspire the diverse designs of the acoustic PT-symmetric system. Moreover, the intriguing effects of exceptional points (EPs) corresponding to the PT phase transition points can also be observed in a passive PT-symmetric system, such as unidirectional invisibility,[20–24] anomalous reflection and refraction,[25–28] unidirectional sound focusing effect,[29] acoustic negative refraction[30] and sound absorption.[31] However, it is still difficult to construct a gain part for an active PT symmetry in the acoustic system, as the gain parts reported always consist of properly controlled loudspeakers,[32,33] interdigital transducers,[34] etc.

Meanwhile, the piezoelectric composite material[35,36] is widely used in many fields as it is a kind of low-cost but practical transducer. The most commonly used composite material consists of a copper baseplate and a piezoelectric ceramic piece attached to the baseplate. It always can be lumped into idealized discrete elements because it is thin enough and the diameter is much smaller than the acoustic wavelength of the frequency interested.[37,38] Then, the piezoelectric composite material with an external circuit can be easily analyzed with the lumped element model.[39] It can be found that the composite material can perform as a negative impedance device with specific external circuits, that is, we can synthesize a kind of gain material into the acoustic field by adjusting the external circuits connected to the piezoelectric composite material.

In this paper, we present an acoustic active PT-symmetric system constructed by a pair of piezoelectric composite plates that are loaded at the side wall of the waveguide with suitably tailored external electrical circuits. Two identical piezoelectric composite plates are controlled by independent external electrical circuits, respectively, which can provide the desired positive or negative resistances. Crucially, the EPs with unidirectional transparency can also be exactly induced in the presented structure. Meanwhile, the PT-broken phases as well as the reverse of the direction of acoustic transparency can be directly observed by adjusting the distance between the gain and loss parts. Our results are expected to open a different route for acoustic wave control and synthesis of EPs.

[†]Corresponding author. E-mail: xyzou@nju.edu.cn

© 2022 Chinese Physical Society and IOP Publishing Ltd 

## 2. Theoretical analysis

The structure of the designed PT-symmetric system is shown in Fig. 1. Here, a gain part and a loss part with settled distance $L$ are placed on the same side of the airborne tube with hard-wall boundaries. The cross-sectional area of the main tube is $S_{\rm m}$, and the area of the gain (loss) part is $S_{\rm a}$ ($S_{\rm b}$). The acoustic pressure and the corresponding velocity of the incident wave and the transmitted wave are ($p^-$, $v^-$) and ($p^+$, $v^+$), respectively. The air density and speed of acoustic wave are $\rho_0$ and $c_0$ in the tube, respectively. To construct an acoustic PT-symmetric system that satisfies the fundamental relation $(PT)\,S(\omega^*)\,(PT) = S^{-1}(\omega)$,[40] where the operator $P$ represents parity reflection, the operator $T$ represents time reversal and $S$ is the scattering matrix of the system, respectively. We take the relationship for the acoustic pressures and velocities of the incident and transmitted waves into consideration because the system can be described as a standard two-port network model, which can be written as

$$\begin{bmatrix} p^- \\ v^- \end{bmatrix} = \begin{bmatrix} A & B \\ C & D \end{bmatrix} \begin{bmatrix} p^+ \\ v^+ \end{bmatrix}, \tag{1}$$

where the $\begin{bmatrix} A & B \\ C & D \end{bmatrix}$ matrix is the total transfer matrix of the designed structure. We divide the structure into two parts, the gain part and the loss part with settled distance $L$ as depicted in Fig. 1, then the total transfer matrix can be expressed as $\begin{bmatrix} A & B \\ C & D \end{bmatrix} = M_{\rm a}M_{\rm T}M_{\rm b}$. Here, $M_{\rm a}$ and $M_{\rm b}$ are the transfer matrixes of the loss part and gain part, respectively, and $M_{\rm T}$ is the transfer matrix of the tube between the two parts. Thus, the transfer matrix can be respectively written as (Appendix A)

$$\begin{aligned} M_{\rm a} &= \begin{bmatrix} 1 & 0 \\ \frac{S_{\rm a}}{Z_{\rm a}S_{\rm m}} & 1 \end{bmatrix}, \quad M_{\rm T} = \begin{bmatrix} \cos x & {\rm j}z_0 \sin x \\ \frac{{\rm j}\sin x}{Z_0} & \cos x \end{bmatrix}, \\ M_{\rm b} &= \begin{bmatrix} 1 & 0 \\ \frac{S_{\rm b}}{Z_{\rm b}S_{\rm m}} & 1 \end{bmatrix}. \end{aligned} \tag{2}$$

As a result, the scattering matrix ($S$) can then be calculated as

$$\begin{aligned} S &= \begin{bmatrix} S_{11} & S_{12} \\ S_{21} & S_{22} \end{bmatrix} = \begin{bmatrix} t^- & r^- \\ r^+ & t^+ \end{bmatrix} \\ &= \begin{bmatrix} \frac{A+\frac{B}{Z_0}-CZ_0-D}{A+\frac{B}{Z_0}+CZ_0+D} & \frac{2(AD-BC)}{A+\frac{B}{Z_0}+CZ_0+D} \\ \frac{2}{A+\frac{B}{Z_0}+CZ_0+D} & \frac{-A+\frac{B}{Z_0}-CZ_0+D}{A+\frac{B}{Z_0}+CZ_0+D} \end{bmatrix}. \end{aligned} \tag{3}$$

As the system being reciprocal, i.e., $t^- = t^+ = t$, we obtain $AD - BC = 1$. We denote $\gamma_1$ and $\gamma_2$ as the normalized quantities $\gamma_1 = \frac{Z_0 S_{\rm a}}{Z_{\rm a} S_{\rm m}}$ and $\gamma_2 = \frac{Z_0 S_{\rm b}}{Z_{\rm b} S_{\rm m}}$, then the scattering parameters can be rewritten in a simplified form (Appendix B).

Generally, a PT-symmetric system shall possess the balanced gain and loss parts, namely, the gain should compensate the loss properly in a PT-symmetric system. In the designed structure, we set $\gamma_1 = -\gamma_2^*$, which means that the normalized impedances of the gain and loss parts are equal with respect to the real part and opposite with the imaginary part. Hence, the fundamental relation $(PT)\,S(\omega^*)\,(PT) = S^{-1}(\omega)$ can be achieved as well. Further, for the synthesis of the PT-symmetric system and seeking the EPs, we calculate the eigenvalues of the scattering matrix as $\lambda_{1,2} = t \pm \sqrt{r^- r^+} = t \times (1 \pm \sqrt{1 - |t|^{-2}})$, from which we can figure out that the system is at the exact PT-symmetric phase when $t < 1$ as the two eigenvalues are unimodular $|\lambda_{1,2}| = 1$. When $t > 1$, the amplitudes of both eigenvalues differ from unity and on both sides respectively, meet the equation $|\lambda_1|\,|\lambda_2| = 1$ at the same time, which corresponds to the broken PT-symmetric phase. Crucially, when $t = 1$, the two eigenstates become degenerate and the system experiences a change from PT exact phase to PT broken phase as it comes to EPs.[10,15]

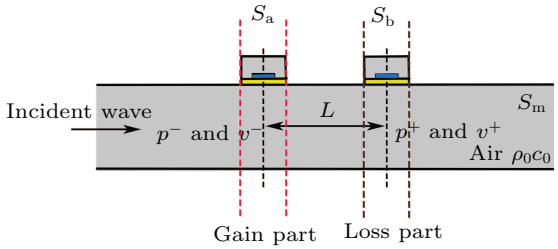



**Fig. 1.** Schematic of the designed PT-symmetric system.

As quantum EPs designed by engineering the Hamiltonian matrix, acoustic EPs can be achieved by manipulating the elements in the corresponding scattering matrix. The system will be in a unidirectional invisible state when it is at EPs, which corresponds to $S_{11} = 0$ when $\gamma_1 = -\gamma_2 = 2$ (Appendix B). In this case, the reflection from the left is zero while it is non-zero from the right. We can substitute $\gamma_1 = -\gamma_2 = \gamma$ ($\gamma$ is real number) into Eq. (3), and obtain the relation as presented in Fig. 2(a). Here, $x = k_0 L$ is the acoustic separation length between the gain and loss parts, we set $x = \arcsin(3/5)$ as the choice of $x$ value does not make much difference to the shapes of the curves. As we can see, only when $\gamma = 2$, the reflection coefficient from the left comes to zero while the reflection coefficient from the other side is non-zero. And the transmission coefficients from both sides are unity at the point. It means that $\gamma = 2$ is the particular situation where the system is at EPs with arbitrary $x$.

Then we consider another nonspecial situation $\gamma = 1 + {\rm j}$. The scattering parameters are shown in Fig. 2(b) with different values of $x$. There are two different zero points at $x = 0.463$ and $x = 1.571$ corresponding to zero reflection coefficient from left and right, respectively. When $x = 0.463$, the reflection from the side of loss part is zero. And when $x = 1.571$, the reflection from the side of gain part is zero. That is to say, the reversal of the direction of the unidirectional invisibility can be found by turning the distance between the two parts. The transmission coefficients at these points have the unity absolute value while the absolute values of the eigenvalues are at

the tipping points, for eigenvalues degenerate or not as can be seen in Fig. 2(c). It means that the two points are both EPs here and the system is at the PT-broken phase when $x$ differs from 0.463 to 1.571.

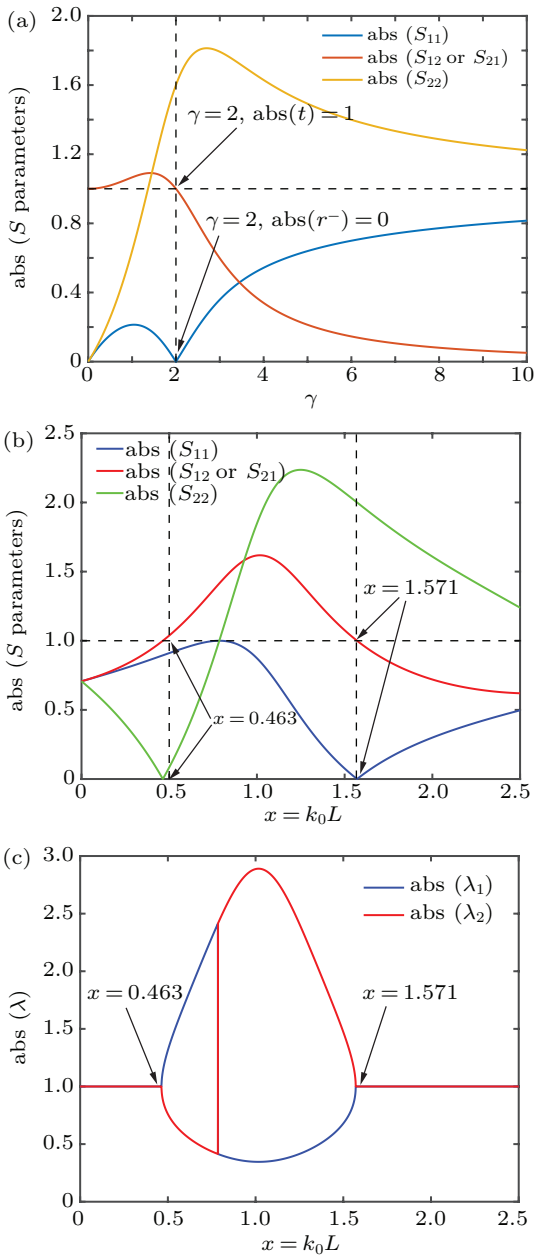



**Fig. 2.** Theoretical results of the scattering parameters and eigenvalues of the scattering matrix. (a) Scattering parameters with different $\gamma$ when $x = \arcsin(3/5)$. Only one EP at $\gamma = 2$ where $S_{11} = 0$ and abs $(S_{12}) = 1$ ('abs' means absolute value). (b) Scattering parameters with different $x$ when $\gamma = 1 + \mathrm{j}$. (c) Eigenvalues of the scattering matrix with different $x$ when $\gamma = 1 + \mathrm{j}$. The two eigenvalues begin to split when $x = 0.463$ and degenerate again when $x = 1.571$. Both the two points are EPs.

To obtain the required normalized acoustic impedance for the gain and loss side branches, the piezoelectric composite plate with an external circuit is introduced. As shown in Fig. 3(a), there is a short tube with the piezoelectric composite plate covering the opening. The tube is used to ensure the external environment of the piezoelectric composite plate. Therefore, the acoustic impedance of this structure can be obtained as the sum of the piezoelectric composite plate and the tube as $Z_{\mathrm{sum}} = Z_{\mathrm{plate}} + Z_{\mathrm{tube}}$. Here, if we consider the end as acoustic hard-wall boundary, $Z_{\mathrm{tube}}$ can be calculated directly by using the impedance transfer equation as $Z_{\mathrm{tube}} \approx -\mathrm{j}\rho_0 c_0 \cot(kh)$, where $h$ is the length of the tube.

As for the piezoelectric composite plate [Fig. 3(a), right panel], it consists of a piece of copper as baseplate and a piece of PZT-5H (with aluminized surface) attached to the middle of the upper surface of the baseplate. We consider that the thickness of the aluminum film is negligible. The radius and thickness of the PZT-5H are $\mathrm{Thk}_1 = 0.21$ mm and $\mathrm{Rad}_1 = 9.5$ mm, respectively. The dimensions of the copper baseplate are $\mathrm{Thk}_2 = 0.13$ mm and $\mathrm{Rad}_2 = 13.5$ mm, respectively. Considering that the dimensions of the plate are much smaller than the wavelengths of the interesting frequencies, the composite plate can thus be lumped into idealized discrete circuit elements around the resonant frequency as illustrated in Fig. 3(b). It can be lumped into two parts: the first part is described as the acoustic domain that includes the acoustic resistance $R_{\mathrm{ap}}$, acoustic mass $M_{\mathrm{ap}}$ and the short-circuit acoustic compliance $C_{\mathrm{ap}}$ of the piezoelectric composite plate; the second part is described as the electrical domain that includes the blocked electrical capacitance $C_{\mathrm{eb}}$ of the piezoelectric diaphragm and the external electrical load impedance $Z_{\mathrm{el}}$ across the piezoelectric composite plate. Between the two parts, there is an approximate lossless transformer with the turn ratio $\phi$ that converts energy between the two domains. Therefore, the blocked electrical capacitance and electrical impedance can be transformed to acoustic domain as $C_{\mathrm{aeb}} = C_{\mathrm{eb}}/\phi^2$ and $Z_{\mathrm{al}} = \phi^2 Z_{\mathrm{el}}$. As a result, we can obtain the simplified equivalent circuit representation by the pure acoustic impedance as shown in Fig. 3(c), and the total acoustic impedance of the plate is given by

$$Z_{\mathrm{plate}} = R_{\mathrm{ap}} + \mathrm{j}\omega M_{\mathrm{ap}} + \frac{1}{\mathrm{j}\omega C_{\mathrm{ap}}} + \frac{Z_{\mathrm{al}}}{1 + \mathrm{j}\omega C_{\mathrm{aeb}} Z_{\mathrm{al}}}, \tag{4}$$

where $\omega = 2\pi f$ is the angular frequency when the operating frequency is $f$. The acoustic impedance of a piezoelectric composite plate is determined once made, while it is feasible to change the whole equivalent acoustic impedance by adjusting the impedance of the external circuit. Thus, active control can be introduced, and we can synthesize the gain part and loss part by linking the negative or positive impedance circuit to the piezoelectric composite plates. To begin with, we should measure the parameters of the piezoelectric composite plate. Here, we put forward a method to determine all the parameters of a piezoelectric composite plate around the resonant frequency by measuring the short-circuit resonant frequency ($f_1$), the open-circuit resonant frequency ($f_2$), and the impedance of the plate with short-circuit external circuit at the open-circuit resonant frequency ($Z_{\mathrm{p0}}$, the real part of $Z_{\mathrm{p0}}$ noted as $Z_{\mathrm{p01}}$, and $Z_{\mathrm{p02}}$ for the imaginary part). The parameters of

the piezoelectric composite plate can be obtained from the following equations (Appendix C):

$$R_{\rm ap} \cong Z_{\rm p01}, \tag{5}$$

$$C_{\rm aeb} = -\frac{1}{{\rm j}\omega_2 Z_{\rm p02}}, \tag{6}$$

$$C_{\rm ap} = -\frac{f_2^2}{f_1^2}\cdot\frac{1}{{\rm j}\omega_2 Z_{\rm p02}} + \frac{1}{{\rm j}\omega_2 Z_{\rm p02}}, \tag{7}$$

$$M_{\rm ap} = \frac{1}{C_{\rm ap}\omega_1^2}\cdot\frac{1}{\left(-\frac{f_2^2}{f_1^2}\cdot\frac{1}{{\rm j}\omega_2 Z_{\rm p02}} + \frac{1}{{\rm j}\omega_2 Z_{\rm p02}}\right)\omega_1^2}. \tag{8}$$

Here, $\omega_1 = 2\pi f_1$ and $\omega_2 = 2\pi f_2$. This method has no need to carefully measure the transverse displacement of the whole plate as the traditional method,[37–39] in which it is hard to measure the lateral displacement accurately and deduce these parameters by integrating with respect to the displacement.

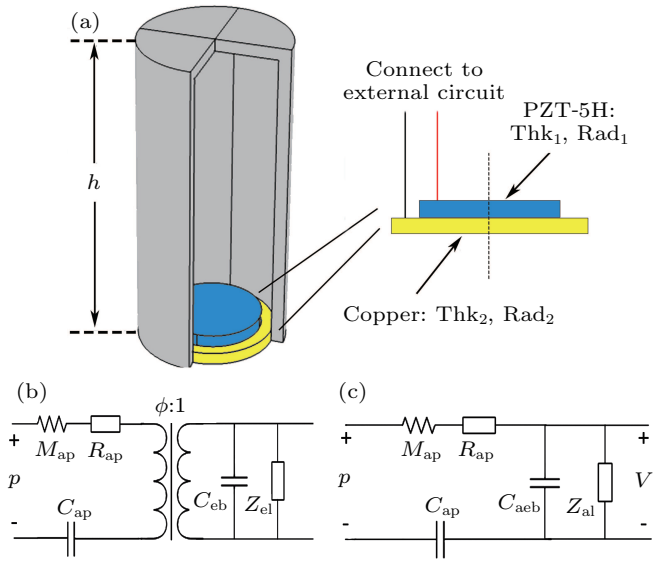



**Fig. 3.** (a) Schematic of a single part loaded at the side of waveguide. (b) Lumped element model of a piezoelectric composite plate with the external circuit load $Z_{\rm el}$. (c) Acoustics analogy circuit diagram to (b) as the electrical domain can transfer to acoustic domain by the transformer with $C_{\rm aeb} = C_{\rm eb}/\phi^2$ and $Z_{\rm al} = Z_{\rm el}\phi^2$.

## 3. Computational results

The acoustic impedances and the reflection coefficients of the piezoelectric composite plate can be obtained from the two-microphone method (TMM).[41] The illustration of the TMM is shown in Fig. 4(a). The distance between the two microphones is $s$, the distance from the surface of the measuring structure to the nearest microphone is $l$, and the frequency response function between Mic. 1 and Mic. 2 is $H_{12}$. Here, the frequency response can also be expressed as the ratio of the complex pressure at Mic. 2 to the complex pressure at Mic. 1. We assume that the effects of tube attenuation and viscosity are negligible, and only plane wave propagates along the tube, then the complex reflection coefficient at the sample surface and its acoustic impedance can be given by

$$R = \frac{p^-}{p^+} = \frac{H_{12} - {\rm e}^{-{\rm j}ks}}{{\rm e}^{{\rm j}ks} - H_{12}}\,{\rm e}^{{\rm j}2k(l+s)}, \tag{9}$$

$$Z_{\rm a} = \rho_0 c_0 \frac{1+R}{1-R}. \tag{10}$$

Then, the acoustic impedances of the piezoelectric composite plate at different frequencies and its resonant frequencies with open or short external circuit can be obtained. With the dimensions proposed above, we get the two resonant frequencies $f_1 = 1755.9$ Hz and $f_2 = 1874.2$ Hz from Figs. 4(b)–4(e). It can be seen that the imaginary part of the specific acoustic impedance comes to zero and the absolute value of the reflection coefficient reaches the minimum value, which agrees well with the theory. And we can get $Z_{\rm p0} = 765882.2 + {\rm j}\cdot 9632156.2$ kg/(m$^4$·s) further. Then, the parameters of the piezoelectric composite plate ($R_{\rm ap}$, $C_{\rm aeb}$, $C_{\rm ap}$, $M_{\rm ap}$) can be obtained (Appendix C). However, the turn ratio $\phi$ is necessary if we want to design the external circuits for different required equivalent acoustic impedance. We choose $f_3 = 1800$ Hz to calculate it. When the plate is shorted-circuited, the corresponding acoustic impedance is $Z_{\rm a1} = 765917 + {\rm j}\cdot 3652139$ kg/(m$^4$·s). Further, we load the plate with $Z_{\rm el0} = 1000\ \Omega$ and then the acoustic impedance is $Z_{\rm a2} = 3989143.5 + {\rm j}\cdot 2441532.5$ kg/(m$^4$·s). Thus, the turn ratio $\phi$ can be obtained by

$$\phi = \sqrt{\frac{Z_{\rm a2} - Z_{\rm a1}}{Z_{\rm el0} - (Z_{\rm a2} - Z_{\rm a1})\,{\rm j}\omega_3 C_{\rm aeb} Z_{\rm el0}}} \cong 60.64, \tag{11}$$

where $\omega_3 = 2\pi f_3$. As shown in Fig. 4(f), the theoretical impedances are relatively accurate around the two resonant frequencies. As a result, we can design the equivalent impedance of the plate with different external circuits.

Considering the special situation when $\gamma_1 = -\gamma_2 = 2$, the main tube section here is square with the inner side length of 27 mm, the side tube section is circular with the inner radius of 13.5 mm, and the heights of the two tubes are all 34 mm in Fig. 6. Thus, the required specific acoustic impedance is $Z_1 = \frac{Z_0 S_{\rm a}}{\gamma_1 S_{\rm m}} \cong 172$ kg/(m$^2$·s) and $Z_2 = \frac{Z_0 S_{\rm a}}{\gamma_2 S_{\rm m}} \cong -172$ kg/(m$^2$·s), respectively. Correspondingly, the electrical load that we need to acquire the special acoustic impedance at the frequency $f_3 = 1800$ Hz can be calculated as

$$Z_{\rm e1} = \frac{Z_{\rm t1}}{\phi^2 - {\rm j}\omega_3 Z_{\rm t1} C_{\rm aeb}\phi^2}, \tag{12}$$

$$Z_{\rm e2} = \frac{Z_{\rm t2}}{\phi^2 - {\rm j}\omega_3 Z_{\rm t2} C_{\rm aeb}\phi^2}, \tag{13}$$

where $Z_{{\rm t}i} = Z_i/s_{\rm a} - Z_{\rm a1} - Z_{\rm tube}$. Since that the electrical load can be expressed as $Z_{\rm e} = R_{\rm e0} + {\rm j}\omega_3 M_{\rm e0}$, the external circuits are then deduced from the relations shown before and can be presented as resistances and inductances as $R_{\rm e0p} =$

$-255.74\ \Omega$, $M_{e0p} = -98.91$ mH for the passive plate and $R_{e0a} = -548.72\ \Omega$, $M_{e0a} = -93.07$ mH for the active plate, respectively. To obtain the negative impedance and inductance, a non-foster circuit is used here as shown in Fig. 5(a). the negative impedance is implemented by an operational amplifier with feedback resistors, and the corresponding equivalent circuit diagram is shown in Fig. 5(b). The effective negative electric impedance at the connector is

$$R_{\text{total}} = -\frac{R_e + j\omega_3 M_e}{R_2} \cdot R_1 = -\frac{R_e R_1}{R_2} - \frac{j\omega_3 M_e R_1}{R_2}, \quad (14)$$

where the resistors are $R_2 = 1$ kΩ and $R_1 = 5$ kΩ for both passive and active piezoelectric composite plates. For the passive plate, $R_{ep} = -R_{e0p}/5 = 51.15\ \Omega$ and $M_{ep} = -M_{e0p}/5 = 19.78$ mH, the corresponding special acoustic impedance of the piezoelectric composite plate is $Z'_{sp} = 170.94 + j \times 3.17\ \text{kg}/(\text{m}^2{\cdot}\text{s})$. For the active plate, $R_{ea} = -R_{e0a}/5 = 109.74\ \Omega$ and $M_{ea} = -M_{e0a}/5 = 18.61$ mH, the corresponding special acoustic impedance of the piezoelectric composite plate is $Z'_{sa} = -169.25 - j1.01\ \text{kg}/(\text{m}^2{\cdot}\text{s})$. These results indicate that the way we used to synthesize the required acoustic impedance by adjusting the external circuit is well-suited as the percentage error being less than 3%.

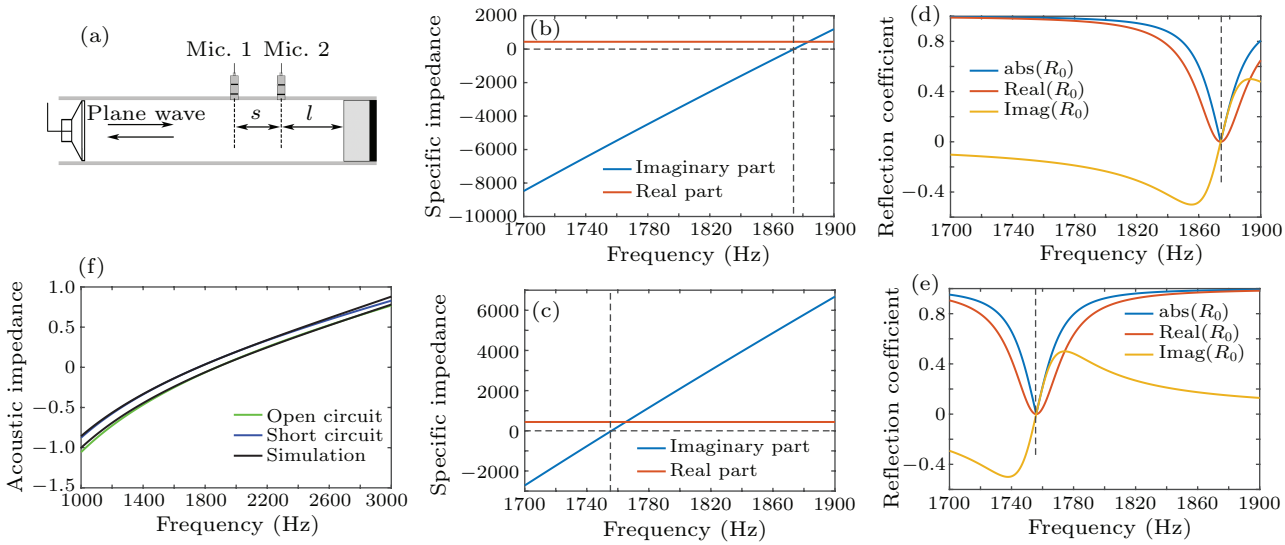



**Fig. 4.** (a) Schematic of the two-microphone method. (b) Specific acoustic impedance near the resonant frequency when the piezoelectric composite plate is open-circuited. (c) Specific acoustic impedance near the resonant frequency when the plate is short-circuited. (d) Reflection coefficient when the plate is open-circuited. (e) Reflection coefficient when the plate is short-circuited. (f) Acoustic impedances of the plate acquired by calculating with the lumped elements.

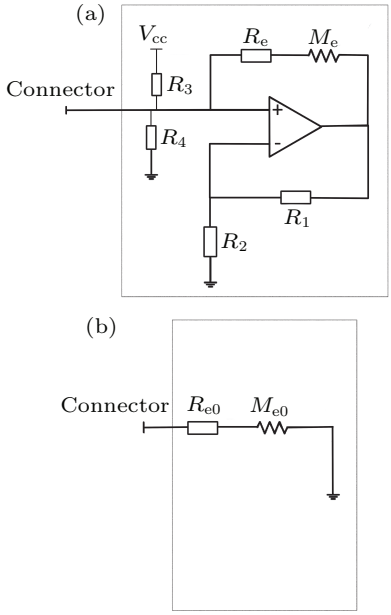



**Fig. 5.** (a) The electronic schematic for external circuits. The resistors $R_3$ and $R_4$ provide the input bias of $V_{cc}/2$ at the positive input of the amplifier. Specifically, $R_3 = R_4 = 100$ kΩ, $R_2 = 1$ kΩ, $R_1 = 5$ kΩ. (b) Equivalent circuit schematic of the circuit, $R_{e0} = -5R_e$, $M_{e0} = -5M_e$.

Further, we combine the passive part and active part for the synthesis of the EP in PT-symmetric system as shown in Fig. 1. The active part is connected to the external circuit as presented in Fig. 5(a) with $R_{ea} = 51.15\ \Omega$ and $M_{ea} = 19.78$ mH, while the passive part is connected to the same circuit with $R_{ep} = 109.74\ \Omega$ and $M_{ep} = 18.61$ mH. And the corresponding acoustic pressure fields of distributions are depicted in Fig. 6. It is clear that the reflected acoustic wave nearly vanishes when the acoustic wave comes from the left of loss part. On the contrary, the reflection coefficient is relatively large when the acoustic wave comes from the right of gain part. These results indicate that the presented PT-symmetric system and the corresponding EPs are consistent with the calculation results and fairly accurate.

Then, we choose $\gamma = 1 - j$ as an example for the nonspecial situation, which corresponds to $Z_1 = 172 - 172j\ \text{kg}/(\text{m}^2{\cdot}\text{s})$ and $Z_2 = -172 - 172j\ \text{kg}/(\text{m}^2{\cdot}\text{s})$. All the other parameters are as the same as the sample discussed above, and we can synthesize the special acoustic impedances directly by merely turning $R_e$ and $M_e$. In this case, the passive part is connected to the external circuit with $R_{ep} = -(280.16/5)\ \Omega = 56.03\ \Omega$ and $M_{ep} = -(115.4/5)$ mH =

23.08 mH, while the active part is connected to the same circuit with $R_{ea} = 124.0\ \Omega$ and $M_{ea} = 21.52$ mH. The measured special acoustic impedance of passive part is $Z'_{sp} = 169.23 - 177.43\mathrm{j}\ \mathrm{kg}/(\mathrm{m}^2{\cdot}\mathrm{s})$, and $Z'_{sa} = -169.03 - 172.30\mathrm{j}\ \mathrm{kg}/(\mathrm{m}^2{\cdot}\mathrm{s})$ for the active part. Crucially, the percentage error here is less than 3% as well. Then we combine the passive part and active part for the synthesis of the EP as shown in Fig. 7. Here we set $x = 1.57$ which is corresponding to the unidirectional transparent point for the wave coming from the left of loss part. The actual reflection coefficient is 0.134 in simulation which is much larger than the coefficient obtained from the particular situation $\gamma = 2$ as the deviation of the distance $L$ and the normalized quantity $\gamma$ both influence the result.

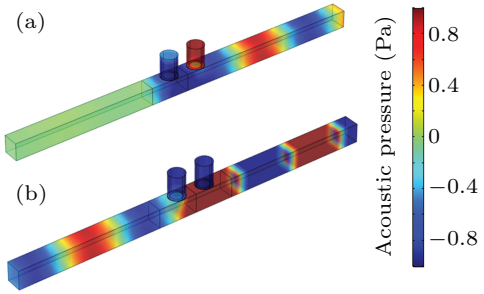



**Fig. 6.** The $\gamma = 2$ is fulfilled thus the system is at EPs with arbitrary value of $L$, and $x = 1.7$ is chosen as an example. (a) Scattering acoustic pressure when the input is coming from the left of loss part. The reflection coefficient here is 0.024 and the frequency of acoustic waves is $f_3 = 1800$ Hz. (b) Scattering acoustic pressure when the input is coming from the right of gain part.

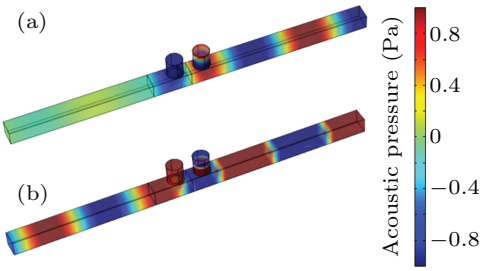



**Fig. 7.** The $\gamma = 1 - \mathrm{j}$ and the system is at EPs when $x = 1.571$ or 2.687, and $x = 1.571$ is chosen as an example. (a) Scattering acoustic pressure when input is coming from the left of loss part. The reflection coefficient here is 0.134 and the frequency of acoustic waves is $f_3 = 1800$ Hz. (b) Scattering acoustic pressure when input is coming from the right of gain part.

## 4. Discussion and conclusion

In summary, we have designed an active-controlled acoustic PT-symmetric system by the piezoelectric composite plates that connect to different active external circuits. Lumped element model is used and all the parameters are determined by a different way without integrating with respect to the lateral displacement as before, which simplifies the design of the external circuits for the synthesis of PT-symmetric system and EPs. We can also obtain different values of the normalized quantity $\gamma$ with the same structure and same frequency by adjusting external circuits of the piezoelectric composite plates. Unidirectional invisibility can be found at EPs, and the spontaneous PT symmetry broken or the reversal of the direction of the unidirectional invisibility can be achieved by turning the distance between gain part and loss part as well. Our study provides an active control method for constructing PT-symmetric system and opens a different route to controlling scattering parameters of acoustic structures.

## Appendix A: Transfer matrix of the system

It is assumed that only plane waves propagate in the pipe, and the pressure and velocity at the left of the middle of loss part are $p_1$ and $v_1$, at the right are $p_2$ and $v_2$; similarly, at the left of the middle of gain part are $p_3$ and $v_3$, at the right are $p_4$ and $v_4$. Then, the relationships between these $p$ and $v$ can be expressed as

$$p_1 = p_2, \quad S_m v_1 = S_m v_2 + S_a p_2 / Z_a, \tag{A1}$$

$$p_3 = p_4, \quad S_m v_3 = S_m v_4 + S_b p_4 / Z_b, \tag{A2}$$

$$p_3 = p_2 \exp(-\mathrm{j}x), \quad v_3 = v_2 \exp(-\mathrm{j}x). \tag{A3}$$

Then, the transfer matrix of the system can be written as $M = M_a M_T M_b$, where

$$M_a = \begin{bmatrix} 1 & 0 \\ \frac{S_a}{Z_a S_m} & 1 \end{bmatrix}, \quad M_T = \begin{bmatrix} \cos x & \mathrm{j}z_0 \sin x \\ \frac{\mathrm{j}\sin x}{Z_0} & \cos x \end{bmatrix},$$

$$M_b = \begin{bmatrix} 1 & 0 \\ \frac{S_b}{Z_b S_m} & 1 \end{bmatrix}.$$

$Z_0 = \rho_0 c_0$ is the specific acoustics impedance of the air in main tube as $\rho_0$ and $c_0$ are air mass density and acoustic velocity in tube, respectively, $x = k_0 L$ is the acoustic separation length between the gain and loss parts with the wave vector $k_0$.

The total transfer matrix can be expressed as

$$M = \begin{bmatrix} A & B \\ C & D \end{bmatrix} = \begin{bmatrix} \cos x + \frac{\mathrm{j}z_0 S_b \sin x}{Z_b S_m} & \mathrm{j}z_0 \sin x \\ \frac{S_a \cos x}{Z_a S_m} + \frac{\mathrm{j}\sin x}{z_0} + \frac{\mathrm{j}z_0 S_a S_b \sin x}{Z_b S_m Z_a S_m} + \frac{S_b \cos x}{Z_b S_m} & \frac{\mathrm{j}z_0 S_a \sin x}{Z_a S_m} + \cos x \end{bmatrix}. \tag{A4}$$

## Appendix B: Simplify the scattering matrix

Note $\gamma_1$ and $\gamma_2$ the normalized quantities $\gamma_1 = \frac{Z_0 S_a}{Z_a S_m}$ and $\gamma_2 = \frac{Z_0 S_b}{Z_b S_m}$, then the scattering matrix of the system can be simplified as

$$S_{11} = \frac{A + \frac{B}{Z_0} - CZ_0 - D}{A + \frac{B}{Z_0} + CZ_0 + D}$$

$$= \frac{-(\gamma_1+\gamma_2)\cos x + \mathrm{j}\,(\gamma_2-\gamma_1-\gamma_1\gamma_2)\sin x}{(2+\gamma_1+\gamma_2)\cos x + \mathrm{j}\,(2+\gamma_1+\gamma_2+\gamma_1\gamma_2)\sin x}, \quad \text{(B1)}$$

$$S_{21} = S_{12} = \frac{2}{A+\frac{B}{Z_0}+CZ_0+D}$$

$$= \frac{2}{(2+\gamma_1+\gamma_2)\cos x + \mathrm{j}\,(2+\gamma_1+\gamma_2+\gamma_1\gamma_2)\sin x}, \quad \text{(B2)}$$

$$S_{22} = \frac{-A+\frac{B}{Z_0}-CZ_0+D}{A+\frac{B}{Z_0}+CZ_0+D}$$

$$= \frac{-(\gamma_1+\gamma_2)\cos x + \mathrm{j}\,(\gamma_1-\gamma_2-\gamma_1\gamma_2)\sin x}{(2+\gamma_1+\gamma_2)\cos x + \mathrm{j}\,(2+\gamma_1+\gamma_2+\gamma_1\gamma_2)\sin x}. \quad \text{(B3)}$$

For any value of $x$, we can get two equations when set $S_{11}=0$,

$$\begin{cases} \gamma_1+\gamma_2=0, \\ \gamma_2-\gamma_1-\gamma_1\gamma_2=0. \end{cases} \quad \text{(B4)}$$

Then unique solution is $\gamma_1=-\gamma_2=2$ for different values of $x$. And when $\gamma_1=-\gamma_2=\gamma$, the scattering matrix can be further simplified as

$$S_{11} = \frac{\mathrm{j}\,(-2\gamma+\gamma^2)\sin x}{2\cos x+\mathrm{j}\,(2-\gamma^2)\sin x}, \quad \text{(B5)}$$

$$S_{21} = S_{12} = \frac{2}{2\cos x+\mathrm{j}\,(2-\gamma^2)\sin x}, \quad \text{(B6)}$$

$$S_{22} = \frac{\mathrm{j}\,(2\gamma+\gamma^2)\sin x}{2\cos x+\mathrm{j}\,(2-\gamma^2)\sin x}. \quad \text{(B7)}$$

Crucially, when $\gamma=2$, $S_{11}=0$, $\mathrm{abs}\,(S_{21})=\mathrm{abs}\,(S_{12})=1$, and $S_{22}=\frac{\mathrm{j}8\sin x}{2\cos x-\mathrm{j}2\sin x}\neq 0$.

## Appendix C: Calculation of the parameters of the piezoelectrical composite plate

When $Z_{\mathrm{AL}}\to 0$, that is, the piezoelectrical composite plate is short-circuited, the total acoustic impedance and the resonant frequency of the plate are

$$Z_{\mathrm{p1}} = R_{\mathrm{ap}}+\mathrm{j}\omega_1 M_{\mathrm{ap}}+\frac{1}{\mathrm{j}\omega_1 C_{\mathrm{ap}}},$$
$$f_1 = \frac{1}{2\pi}\frac{1}{\sqrt{C_{\mathrm{ap}}M_{\mathrm{ap}}}}. \quad \text{(C1)}$$

When the plate is open-circuited as $Z_{\mathrm{AL}}\to\infty$, the total acoustic impedance and resonant frequency are

$$Z_{\mathrm{p2}} = R_{\mathrm{ap}}+\mathrm{j}\omega_2 M_{\mathrm{ap}}+\frac{1}{\mathrm{j}\omega_2 C_{\mathrm{ap}}}+\frac{1}{\mathrm{j}\omega_2 C_{\mathrm{aeb}}},$$
$$f_2 = \frac{1}{2\pi}\frac{1}{\sqrt{C_{||}M_{\mathrm{ap}}}}. \quad \text{(C2)}$$

Here, $C_{||}=C_{\mathrm{ap}}C_{\mathrm{aeb}}/(C_{\mathrm{ap}}+C_{\mathrm{aeb}})$. The acoustic impedance can be obtained by the two-microphone method and the resonant frequency is corresponding to zero imaginary part of the acoustic impedance.

At the short-circuit resonant frequency, we can get

$$\mathrm{j}\omega_1 M_{\mathrm{ap}}+\frac{1}{\mathrm{j}\omega_1 C_{\mathrm{ap}}}=0. \quad \text{(C3)}$$

At the open-circuit resonant frequency, we can get

$$\mathrm{j}\omega_2 M_{\mathrm{ap}}+\frac{1}{\mathrm{j}\omega_2 C_{\mathrm{ap}}}+\frac{1}{\mathrm{j}\omega_2 C_{\mathrm{aeb}}}=0. \quad \text{(C4)}$$

The impedance of the plate with short-circuit external circuit at the open-circuit resonant frequency is $Z_{\mathrm{p0}}$,

$$Z_{\mathrm{p0}} = R_{\mathrm{ap}}+\mathrm{j}\omega_2 M_{\mathrm{ap}}+\frac{1}{\mathrm{j}\omega_2 C_{\mathrm{ap}}} = Z_{\mathrm{p01}}+\mathrm{j}Z_{\mathrm{p02}}. \quad \text{(C5)}$$

From Eq. (C4),

$$\mathrm{j}\omega_2 M_{\mathrm{ap}}+\frac{1}{\mathrm{j}\omega_2 C_{\mathrm{ap}}} = -\frac{1}{\mathrm{j}\omega_2 C_{\mathrm{aeb}}}. \quad \text{(C6)}$$

Then we can get $R_{\mathrm{ap}}=Z_{\mathrm{p01}}$, $C_{\mathrm{aeb}}=-1/\mathrm{j}\omega_2 Z_{\mathrm{p02}}$. Substitute $C_{\mathrm{aeb}}$ into Eqs. (C1) and (C2), we can calculate the value of $C_{\mathrm{ap}}$ as

$$C_{\mathrm{ap}} = \frac{f_2^2}{f_1^2}\cdot C_{\mathrm{aeb}} - C_{\mathrm{aeb}} = -\frac{f_2^2}{f_1^2}\cdot\frac{1}{\mathrm{j}\omega_2 Z_{\mathrm{p02}}}+\frac{1}{\mathrm{j}\omega_2 Z_{\mathrm{p02}}}. \quad \text{(C7)}$$

Substitute $C_{\mathrm{ap}}$ into Eq. (C1),

$$M_{\mathrm{ap}} = \frac{1}{C_{\mathrm{ap}}\omega_1^2}\frac{1}{\left(-\frac{f_2^2}{f_1^2}\cdot\frac{1}{\mathrm{j}\omega_2 Z_{\mathrm{p02}}}+\frac{1}{\mathrm{j}\omega_2 Z_{\mathrm{p02}}}\right)\omega_1^2}. \quad \text{(C8)}$$

With these equations above, the parameters of the plate we used in this paper can then be calculate as

$$C_{\mathrm{aeb}} = 8.8160\times10^{-12}\ \mathrm{m^4\cdot s^2/kg},$$
$$C_{\mathrm{ap}} = 1.2276\times10^{-12}\ \mathrm{m^4\cdot s^2/kg},$$
$$M_{\mathrm{ap}} = 6.6923\times10^{-3}\ \mathrm{kg/m^4}. \quad \text{(C9)}$$

## Acknowledgements

Project supported by the National Key R&D Program of China (Grant No. 2017YFA0303700), the National Natural Science Foundation of China (Grant Nos. 11634006, 11934009, and 12074184), the Natural Science Foundation of Jiangsu Province, China (Grant No. BK20191245), and the State Key Laboratory of Acoustics, Chinese Academy of Sciences.

## References

[1] Bender C M and Boettcher S 1998 *Phys. Rev. Lett.* **80** 5243
[2] Bender C M, Boettcher S and Meisinger P N 1999 *J. Math. Phys.* **40** 2201
[3] El-Ganainy R, Makris K G, Christodoulides D N and Musslimani Z H 2007 *Opt. Lett.* **32** 2632
[4] Feng L, Xu Y L, Fegadolli W S, Lu M H, Oliveira J E B, Almeida V R, Chen Y F and Scherer A 2013 *Nat. Mater.* **12** 108
[5] Lin Z, Ramezani H, Eichelkraut T, Kottos T, Cao H and Christodoulides D N 2011 *Phys. Rev. Lett.* **106** 213901
[6] Longhi S 2010 *Phys. Rev. A* **82** 031801
[7] Sun Y, Tan W, Li H, Li J and Chen H 2014 *Phys. Rev. Lett.* **112** 143903
[8] Zhao H, Fegadolli W S, Yu J K, Zhang Z F, Ge L, Scherer A and Feng L 2016 *Phys. Rev. Lett.* **117** 193901
[9] Feng L, Ayache M, Huang J, Xu Y L, Lu M H, Chen Y F, Fainman Y and Scherer A 2011 *Science* **333** 729

[10] Gupta S K, Zou Y, Zhu X Y, Lu M H, Zhang L J, Liu X P and Chen Y F 2019 *Adv. Mater.* **32** 1903639

[11] Rüter C E, Makris K G, El-Ganainy R, Christodoulides D N, Segev M and Kip D 2010 *Nat. Phys.* **6** 192

[12] Feng L, Wong Z J, Ma R M, Wang Y and Zhang X 2014 *Science* **346** 972

[13] Poshakinskiy A V, Poddubny A N and Fainstein A 2016 *Phys. Rev. Lett.* **117** 224302

[14] Jing H, Ozdemir S K, Lu X Y, Zhang J, Yang L and Nori F 2014 *Phys. Rev. Lett.* **113** 053604

[15] Zhu X F, Ramezani H, Shi C Z, Zhu J and Zhang X 2014 *Phys. Rev. X* **4** 031042

[16] Tian Y, Ge H, Lu M H and Chen Y F 2019 *Acta Phys. Sin.* **68** 194301 (in Chinese)

[17] Zhu X Y, Xu Y L, Zou Y, Sun X C, He C, Lu M H, Liu X P and Chen Y F 2016 *Appl. Phys. Lett.* **109** 111101

[18] Wang X, Fang X S, Mao D, Jing Y and Li Y 2019 *Phys. Rev. Lett.* **123** 214302

[19] Merkel A, Romero-Garcia V, Groby J P, Li J and Christensen J 2018 *Phys. Rev. B* **98** 201102

[20] Shen C, Li J F, Peng X Y and Cummer S A 2018 *Phys. Rev. Mater.* **2** 125203

[21] Auregan Y and Pagneux V 2017 *Phys. Rev. Lett.* **118** 174301

[22] Li H X, Rosendo-Lopez M, Zhu Y F, Fan X D, Torrent D, Liang B, Cheng J C and Christensen J 2019 *Research* **2019** 8345683

[23] Ji W Q, Wei Q, Zhu X F, Wu D J and Liu X J 2019 *Europhys. Lett.* **125** 58002

[24] Chen Z, Negahban M, Li Z and Zhu J Y 2020 *J. Phys. D-Appl. Phys.* **53** 095503

[25] Diaz-Robio A and Tretyakov S A 2017 *Phys. Rev. B* **96** 125409

[26] Wang X, Fang X S, Mao D X, Jing Y and Li Y 2019 *Phys. Rev. Lett.* **123** 214302

[27] Liu T, Ma G C, Liang S J, Gao H, Gu Z M, An S W and Zhu J 2020 *Phys. Rev. B* **102** 014306

[28] Wu J Y, Wu X H, Yang X B and Li H Y 2019 *Chin. Phys. B* **28** 104208

[29] Liu T, Zhu X F, Chen F, Liang S J and Zhu J 2018 *Phys. Rev. Lett.* **120** 124502

[30] Lan J, Zhang X W, Wang L, Lai Y and Liu X Z 2020 *Sci. Rep.* **10** 10794

[31] Achilleos V, Theocharis G, Richoux O and Pagneux V 2017 *Phys. Rev. B* **95** 144303

[32] Shi C Z, Dubois M, Chen Y, Cheng L, Ramezani H, Wang Y and Zhang X 2016 *Nat. Commun.* **7** 11110

[33] Fleury R, Sounas D and Alu A 2015 *Nat. Commun.* **6** 5905

[34] Shao L B, Mao W B, Maity S, Sinclair N, Hu Y W, Yang L and Loncăr M 2020 *Nat. Electron.* **3** 267

[35] He Z H, Zhao J B, Yao H, Jiang J N and Chen X 2019 *Acta Phys. Sin.* **68** 134302 (in Chinese)

[36] Wang J W, Wang G, Chen S B and Wen J H 2012 *Chin. Phys. Lett.* **29** 064302

[37] Prasad S, Gallas Q, Horowitz S, Homeijer B, Sankar B V, Cattafesta L N and Sheplak M 2006 *AIAA J.* **44** 2311

[38] Liu F, Horowitz S, Lou C and Sheplak M 2006 *12th Aiaa/ceas Aeroacoustics Conference*, May 8, 2006, Cambridge, MA

[39] Liu F, Horowitz S, Nishida T, Cattafesta L and Sheplak M 2007 *J. Acoust. Soc. Am.* **122** 291

[40] Chong Y D, Ge L and Stone A D 2012 *Phys. Rev. Lett.* **108** 269902

[41] ISO Standard 10534–2 1998 *International Organization for Standardization*